A Two-Stage Stochastic Optimization Model for Air Traffic Conflict Resolution under Wind Uncertainty

Adan E. Vela, Erwan Salaün, Senay Solak†, Eric Feron, William Singhose, John-Paul Clarke
Georgia Institute of Technology, Atlanta, GA
†University of Massachusetts, Amherst, MA

Abstract

This paper considers the air traffic conflict resolution problem in the context of wind uncertainty. Aircraft are assigned changes in airspeed to prevent conflict. The goal is to determine the optimal maneuver to balance deviation costs (e.g., fuel costs) and the probability of conflict. A two-stage recourse model is developed, in which new airspeeds are assigned in the first stage, based on expected costs due to possible corrective actions in the second stage. The second-stage considers the expected costs for any last-minute maneuvers to compensate wind modeling errors. The resulting model is solved in real-time via numerical methods, providing optimal airspeed values for the resolution of a conflict.

Introduction

There has been significant research in the fields of air traffic conflict detection and conflict resolution. A summary of results in both research areas is available in [1]. One key factor in conflict detection and resolution is the uncertainty in present and future estimations of the velocity and position vectors of aircraft. These uncertainties may be due to sensor noise (e.g., error in radar systems) or due to unpredictable disturbances such as wind. Many conflict detection algorithms account for this uncertainty [2], [3], [4]. On the other hand, only limited research has been done on stochastic air traffic conflict resolution [5], [6], [7]. Given the limited literature on conflict resolution under uncertainty, some studies concerned with developing probabilistic conflict detection models conclude by stating that there is a need to better understand and utilize conflict probability estimations in conflict resolution algorithms [8]. Hence, there is a clear need for fully developed and more complete probability based methods for conflict resolution.

In this study, we try to fill this gap by developing a comprehensive stochastic conflict resolution model for a pair of aircraft. To characterize the uncertainty in aircraft trajectories, we consider a linearly growing along-track positional uncertainty measure for aircraft, which is primarily a result of wind disturbances. Such an assumption can be validated by experimental data and a specific auto-correlation function for the along-track wind error. This assumption enables presentation of the conflict resolution problem through a clear and simple geometrical approach, with an analytical expression of the probability of conflict as a function of the airspeed change. The approach draws ideas from [9] and [10].

Similar to the approach in [9] for determining the probability of conflict, it is possible to build a geometrical and analytical two-stage stochastic optimization model to determine the optimal maneuver to prevent conflicts, taking into account the cost of maneuvers and the resulting probability of conflict. Clearly, independent minimization of each of these two criteria leads to conflicting solutions. Hence, we minimize a global cost function that considers a compromise, while constrained by aircraft specifications (e.g., minimal and maximal airspeed changes).

The optimization model is presented as a two-stage stochastic model, where only speed changes are made to resolve conflicts. The first stage considers costs associated with an initial deviation in airspeed. The second stage considers the expected costs associated with any last-minute speed commands required to prevent conflict due to unmodeled wind uncertainties. The resulting formulation withholds from only utilizing arbitrary risk measures such as minimum conflict probabilities or mixed-cost weightings, as the first and second stage costs can be posed in the same units.

The remainder of this paper is structured as follows. First, we present the geometric analysis of the problem considering the effect of uncertainty. In the next section, we characterize the probability of conflict between two aircraft, followed by the two-stage stochastic optimization model. Then we analyze the structure of the

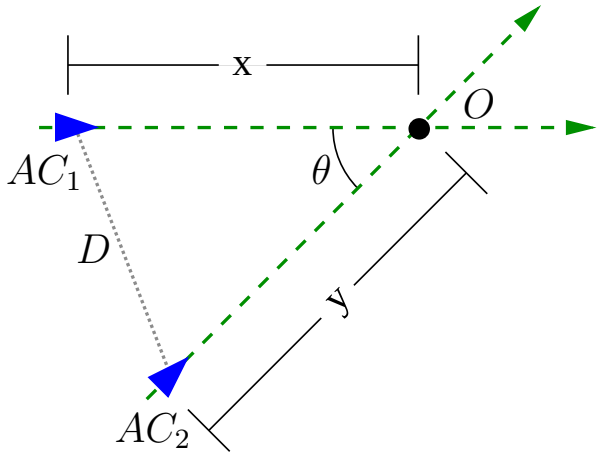

Figure 1: The encounter model is defined by the intersection angle, the speeds and the distances of the aircraft to the intersection

problem from a computational perspective, and present the results from a sample simulation study. Conclusions and future works are discussed at the end of the paper.

Geometric modeling of aircraft conflicts

We first present a geometric representation of the conflict resolution problem, and then discuss how the uncertainty due to wind can be included in this geometric framework.

Encounter modeling

To model the encounter between two aircraft, we use an approach similar to the work presented in [9] and [11]. Consider an intersection between two aircraft trajectories, AC_1 and AC_2 flying along straight-line trajectories and crossing at the point O as shown in Fig. 1. The encounter is defined by the following characteristics:

- θ, the crossing angle
- $\mathbf{d} = [x, y]$, the vector composed of the distances of the two aircraft to the crossing point of the aircraft
- $\mathbf{v}_g = [v_{1,g}, v_{2,g}]$, the groundspeed vector of the aircraft pair
- D_{min}, the minimum separation distance required between two aircraft

The position of the aircraft at some time t is shown in Fig. 1. A conflict between the aircraft exists if the distance between the aircraft, D, is less than D_{min} at any time. Through application of the law of cosines, the

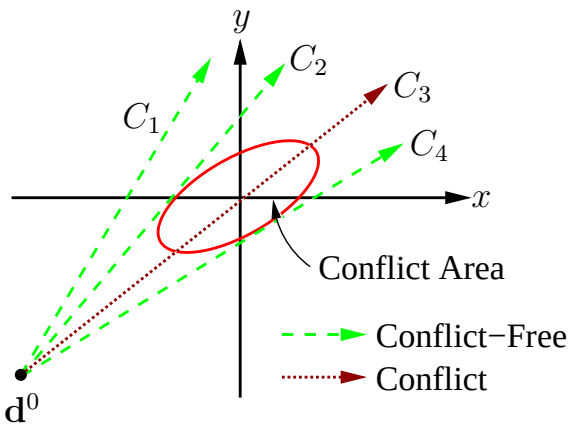

Figure 2: Four different configurations corresponding to different speed-ratios between aircraft

distance constraint between the aircraft can be calculated as:

$$D^2 = x^2 + y^2 - 2xy\cos\theta \geq D_{min}^2. \quad (1)$$

For a given crossing angle θ, when the condition is at equality, i.e. when $D = D_{min}$, it is considered to be the critical configuration.

Since the path of each aircraft is linear, the evolution of the encounter, i.e. ,the position of both aircraft in space, can be represented by a phase-portrait as in Fig. 2. The coordinates of a point in the phase-portrait correspond to the distances x and y of the aircraft from the crossing point. As time progresses, the state of the system will traverse a trajectory from the lower left-hand quadrant to the upper right-hand quadrant. Furthermore, assuming that the aircraft fly with constant speeds, $v_{1,g}$ and $v_{2,g}$, the state trajectory on the phase portrait is a straight line with slope m, where

$$m = \frac{dy}{dx} = \frac{dy/dt}{dx/dt} = \frac{v_{2,g}}{v_{1,g}}$$

In Fig. 2, four lines are plotted corresponding to four different configurations, C_i, with the same initial condition $\mathbf{d}^0 = [x_0, y_0]$, but different speed-ratios, m_i, $i = 1, \ldots, 4$. Figure 2 also contains an ellipsoid, which is described by Eq. (1) and corresponds to the critical configuration when the distance between aircraft is equal to the minimum separation distance D_{min}. Clearly, if the state trajectory remains outside the ellipsoid, then there is no conflict (case C_1), whereas a conflict occurs if the state trajectory passes through the ellipsoid (case C_3). The critical speed-ratios occur when the trajectory and the ellipsoid are tangent (cases C_2 and C_4).

For initial conditions $\mathbf{d}^0$ and $\mathbf{v}_g^0$, conflict will occur if the speed-ratio is such that

$$m_l^c < m = \frac{v_{2,g}^0}{v_{1,g}^0} < m_u^c \tag{2}$$

where m_u^c and m_l^c are the maximum lower-slope and minimum upper-slope required for conflict-free travel, corresponding to the cases C_2 and C_4, respectively. The values of m_l^c and m_u^c represent solutions of m to the following system of equations:

$$\begin{aligned} m &= \frac{y_0 - y}{x_0 - x} \\ x^2 + y^2 - 2xy\cos\theta &= D_{min}^2 \\ \frac{d}{dt}\left(x^2 + y^2 - 2xy\cos\theta\right) &= 0 \\ \frac{dy}{dx} &= m \end{aligned} \tag{3}$$

Expressions for m_l^c and m_u^c can be explicitly derived as a function of x_0, y_0, D_{min}, and θ.

Aircraft and wind uncertainty modeling

Given this geometric framework, we can develop a probabilistic model in order to capture the uncertainty in the conflict between the two aircraft. Due to aircraft performance envelopes and Air Traffic Control (ATC) restrictions, the aircraft are limited in the speed change maneuvers performed to prevent possible conflicts. Assume that aircraft AC_i has a minimum airspeed v_i^{min} and a maximum airspeed v_i^{max}:

$$v_i^{min} \le v_i \le v_i^{max}, \qquad i = 1,2 \tag{4}$$

where the airspeed v_i can directly be related to the groundspeed $v_{i,g}$ through any local wind $v_{i,w}$, as:

$$v_{i,g} = v_i + v_{i,w}, \qquad i = 1,2 \tag{5}$$

For the problem at hand, aircraft will be assigned new airspeeds, v_i^+, to resolve conflicts. However, we will make use of both the groundspeed and airspeed variables throughout the formulation.

If an air traffic controller anticipates a conflict, as determined through a trajectory prediction tool estimating the future positions of the aircraft, avoidance maneuvers can be issued. From radar measurements (or GPS navigation solutions), the position of aircraft AC_i at time t_0 is $(x(t_0), y(t_0))$. The initial position is known within some uncertainty envelope. However, when the aircraft is traveling along a straight path the estimate of the aircraft position may be subject to along-track and cross-track errors with respect to the planned trajectory. With the advent of modern Flight Management Systems (FMS) and pilot corrective actions, the magnitude of any cross-track errors remains small. On the contrary, along-track errors are much more significant and tend to grow with time. In fact, since throttle compensation for regulating groundspeed due to unexpected wind changes is fuel-inefficient and of little use, the FMS and the pilot aim to maintain a constant airspeed, while the actual groundspeed will typically vary with time according to the wind speed. Hence, the predicted groundspeed of the aircraft is dependent on an unpredictable parameter, and so is the predicted position of the aircraft. Due to errors in the modeling of the space and time-varying wind speed, the along-track error can be significant.

Following the previous assumptions, we only consider the along-track error $e_i(\tau)$, where τ is the prediction time. The error $e_i(\tau)$ is the difference between the actual along-track distance $s_i(\tau)$ flown by the aircraft AC_i after time t_0 and the planned (or predicted) along-track distance $\hat{s}_i(\tau)$:

$$e_i(\tau) = \hat{s}_i(\tau) - s_i(\tau) \qquad i = 1,2 \tag{6}$$

According to [10] and [11], the along-track error $e_i(\tau)$ may be modeled as a normally distributed random variable with a standard deviation growing linearly with time:

$$e_i(\tau) = r_i \tau \mathcal{N}_i(0,1) \qquad i = 1,2 \tag{7}$$

where r is the rate of growth of the standard deviation of $e_i(\tau)$ and $\mathcal{N}_i(0,1)$ is a Gaussian distributed variable with zero mean and unit variance. This along-track error model has been validated in [12] by comparing the estimates with real data. Using these results, the rate of growth of the standard deviation is evaluated to be 0.25NM/min. Another approach to justify (7) is to model the wind uncertainty, as it is the dominant cause for any along-track error. Assuming a specific auto-correlation function for the wind along-track speed error, the expression in (7) can be recovered for the position error (see [13] and [14] for details). The auto-correlation function considers that wind speed errors close in time (i.e. for small prediction time τ) are highly correlated,

whereas they become less correlated as the prediction time τ increases, which is sensible from a physical viewpoint. If we rewrite (6)–(7) in terms of speed, we obtain:

$$V_{i,g} = \hat{v}_{i,g} + r_i \mathcal{N}_i(0,1), \qquad i = 1,2 \tag{8}$$

where $V_{i,g}$ is the random variable for the groundspeed, and $\hat{v}_{i,g}$ is the planned (or estimated) groundspeed of the aircraft according to (5).

Probability of conflict

Given a stochastic representation of ground speed, it is possible to derive a relationship for the probability of conflict between two aircraft under known initial conditions. In this section, we describe this relationship, and discuss how changes in airspeed can impact this probabilistic model.

According to (2), a conflict occurs if the speed-ratio $\frac{V_{2,g}}{V_{1,g}}$ lies between m_l^c and m_u^c, where m_l^c and m_u^c are constant parameters for a given encounter configuration (i.e., crossing angle, aircraft departure points and minimal separation distance). Using (8), we can write the random variable M, which represents the stochastic speed-ratio of the aircraft:

$$M = \frac{V_{2,g}}{V_{1,g}} = \frac{\hat{v}_{2,g} + r_2 \mathcal{N}_2(0,1)}{\hat{v}_{1,g} + r_1 \mathcal{N}_1(0,1)} \tag{9}$$

The probability density function of M corresponds to the ratio of two normally distributed random variables with correlation ρ, and is given by [15] as:

$$\begin{aligned} f_M(m) = {} & \frac{b(m)\,d(m)}{\sqrt{2\pi} r_1 r_2 a^3(m)} \left[\Phi\left(\frac{b(m)}{a(m)\sqrt{1-\rho^2}} \right) \right. \\ & \left. -\Phi\left(-\frac{b(m)}{a(m)\sqrt{1-\rho^2}} \right) \right] \\ & + \frac{\sqrt{1-\rho^2}}{\pi r_1 r_2 a^2(m)} exp\left(-\frac{c}{2(1-\rho^2)} \right) \end{aligned} \tag{10}$$

where,

$$\begin{aligned} a(m) &= \left(\left(\frac{m}{r_2} \right)^2 - \frac{2\rho m}{r_1 r_2} + \left(\frac{1}{r_1} \right)^2 \right)^{\frac{1}{2}} \\ b(m) &= \frac{\hat{v}_{2,g} m}{(r_2)^2} - \frac{\rho\,(\hat{v}_{2,g} + \hat{v}_{1,g} m)}{r_1 r_2} + \left(\frac{\hat{v}_{1,g}}{(r_1)^2} \right) \\ c &= \frac{\hat{v}_{2,g}}{(r_2)^2} - \frac{2\rho \hat{v}_{2,g} \hat{v}_{1,g}}{r_1 r_2} + \left(\frac{\hat{v}_{1,g}}{(r_1)^2} \right) \\ d(m) &= \exp\left\{ \frac{b^2(m) - c a^2(m)}{2(1-\rho^2) a^2(m)} \right\} \end{aligned} \tag{11}$$

and $\Phi(x) = \int_{-\infty}^{x} \left(1/\sqrt{2\pi}\right) e^{-\frac{1}{2}u^2} du$. Note that the distribution is defined according to $\hat{\mathbf{v}}_g = [\hat{v}_{1,g} \hat{v}_{2,g}]$, r_1, r_2, and ρ.

Given that $\hat{v}_{i,g}/r_i \gg 0$ and $P(V_{1,g} < 0) \sim 0$, we can make the following approximation:

$$\hat{f}_M(m) = \frac{b(m)\,d(m)}{\sqrt{2\pi} r_1 r_2 a^3(m)} \tag{12}$$

For future calculations we will make use of $\hat{f}_M(m)$ whenever $f_M(m)$ is required.

The approximation that yields (12) uses the assumption that $P(V_{1,g} < 0) \sim 0$. Practically, the condition $\}V_{1,g} < 0\}$ would never occur. It implies that aircraft are flying in winds greater than the airspeed of the aircraft, and hence, it would never reach its destination. In addition, from a cost perspective, this is clearly not a reasonable solution for airline operators.

Two-stage Stochastic Optimization Model

The two-stage stochastic optimization model presents a methodology for capturing uncertainty in the conflict resolution problem by accounting for recourse actions. We assume that the decision process consists of issuing first-stage speed adjustment commands to aircraft in conflict, followed by any necessary second-stage speed adjustments upon realization that a recourse action is required due to conflict.

Note that we only consider aircraft speed changes, and not heading changes, to avoid possible conflicts. The speed changes are made such that the expected two-stage cost function over the decision variables $\mathbf{v}^+$ is minimized. More specifically, the initial airspeeds v_1^0

and v_2^0 change to v_1^+ and v_2^+, where the new speed values still satisfy (4). Any changes in airspeed can be directly linked to the planned groundspeed, $\hat{\mathbf{v}}_g$. As a result, the initial planned speed-ratio m^0 will be updated to the new planned speed-ratio $\hat{m}^+ = \frac{\hat{v}_{2,g}^+}{\hat{v}_{1,g}^+}$.

The motivation behind the two-stage model is as follows. En route aircraft prefer to restrict speed changes to maintain fuel economy and to limit the need for re-submitting flight plans. Overall, aircraft resolution maneuvers can be classified into two categories: (1) conservative commands which guarantee conflict-free flight at the cost of increased fuel-costs, (2) commands that reduce initial fuel-costs, however, increase the probability of requiring additional maneuvers to resolve conflict. Of these, additional last-minute maneuvers typically incur costs at a greater expense than the equivalent first-stage decision. The proposed two-stage stochastic formulation works towards balancing the cost between overly-conservative and overly-risky conflict resolution solutions.

The second-stage speed adjustments are predetermined for each recourse situation, and do not need to be considered as decision variables. However, this requires explicit generation of possible action-recourse processes and the associated costs. We address these issues in the next subsections. To this end, we first consider a single-stage decision process without recourse and describe the corresponding formulation in deterministic and stochastic settings. Then, the two-stage formulation is systematically developed by including recourse actions, restrictions due to aircraft dynamics and cost function calculations.

Deterministic and Stochastic Single-Stage Problems

Consider again the case with two aircraft with crossing trajectories as described previously and illustrated in Fig. 1. Given no uncertainty in wind, the ground speed of the aircraft can be calculated exactly. Hence, the problem reduces to assigning feasible airspeeds, $\mathbf{v}^+$, to the aircraft such that some cost function is minimized. Assuming generic cost functions $g_i(v_i^+)$ for each aircraft,

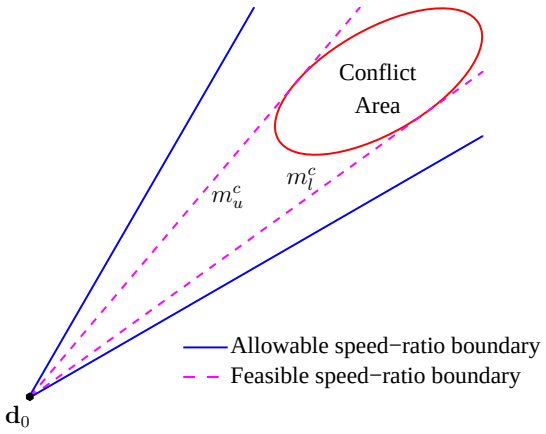

Figure 3: Phase portrait representation of the standard deterministic formulation

this problem can be expressed as follows:

$$\begin{aligned} \text{minimize} \quad & g_1(v_1^+) + g_2(v_2^+) \\ \text{s.t.} \quad & \\ & v_1^{min} \le v_1^+ \le v_1^{max} \\ & v_2^{min} \le v_2^+ \le v_2^{max} \\ & \hat{v}_{1,g} = v_1^+ + v_{1,w} \\ & \hat{v}_{2,g} = v_2^+ + v_{2,w} \\ & \hat{m}^+ = \frac{\hat{v}_{2,g}}{\hat{v}_{1,g}} \\ & \hat{m}^+ \le m_l^c \text{ or } m_u^c \le \hat{m}^+ \end{aligned} \tag{13}$$

Again, v_1^+ and v_2^+ are the assigned airspeeds of the aircraft, and $\hat{m}^+$ is the new speed-ratio for the system. The bounds on v_1^+ and v_2^+ mean that $\hat{m}^+$ is bounded as well. The domain for $\hat{m}^+$ is given by the closed interval $\left[v_{2,g}^{min}/v_{1,g}^{max}, v_{2,g}^{max}/v_{1,g}^{min}\right] = \left[(v_2^{min}+v_{2,w})/(v_1^{max}+v_{1,w}), (v_2^{max}+v_{2,w})/(v_1^{min}+v_{1,w})\right]$. In Fig. 3, the two solid lines emanating from intial aircraft state $\mathbf{d}^0$ represent these bounds on the speed-ratio. Hence, the set of feasible solutions corresponds to the area between these solid lines and the dashed critical speed-ratio lines defined by m_u^c and m_l^c.

Similar to this deterministic formulation, we can develop a single-stage stochastic formulation of the problem based on an $\alpha-$bounded conflict probability, where the feasible space of airspeeds is restricted such that the probability of any first-stage conflict is less than α. Let the average wind over a measurable distance be bounded such that realizable speed-ratios are also bounded. In this case, the problem becomes:

$$\begin{aligned} \text{minimize } & g_1(v_1^+) + g_2(v_2^+) \\ \text{s.t.} \quad (v_1^+, v_2^+) \in \; & \{(v_1, v_2) | P(m_l^c \le M \le m_u^c \\ & | v_1^+ = v_1, v_2^+ = v_2) \le \alpha\} \end{aligned} \tag{14}$$

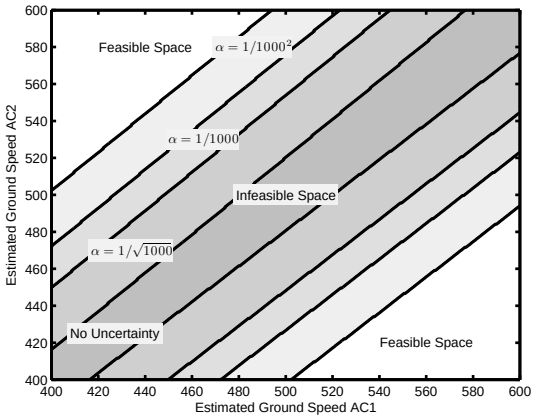

Figure 4: Feasible region for a single-stage stochastic problem

where the speed-ratio M is the random variable described by (9) according to v_1^+, v_2^+ and $v_{1,w}$, $v_{2,w}$.

Examples of the feasible solution space as described by the constraints in deterministic problem (13) and stochastic problem (14) are shown in Fig. 4 for $\alpha = \left\{1/\sqrt{1000}, 1/1000, 1/1000^2\right\}$, and also the deterministic case with no uncertainty. The infeasible solutions for the deterministic case are located within the narrowest band; the size of the infeasible area and expands outwards with decreasing α. In this instance, each aircraft is assumed to be initially $90NM$ from the intersection, with a speed range of $[400, 600]$ kts.

Solution Space to the Two-Stage Stochastic Model

The two-stage model can be constructed by enumerating the solution space according to possible trajectories (no-conflict and conflict-recourse). Figure 5 pictorially defines these trajectories. Given the initial state of the system, $\mathbf{d}^0$ and $\mathbf{v}^0$, aircraft are issued a resolution command $\mathbf{v}^+$. According to the commanded airspeed and random wind input into the system, there are two classes of possible outcomes: **Case 1**-The aircraft reach a point such that it is determined the probability of conflict is low. In this case, the state trajectory intersects with the optimal-horizon line, l_u^{opt} or l_l^{opt}, which defines the set of switching-states where the aircraft may return to the desired or optimal airspeed without concern for conflict, thereby terminating the conflict problem. **Case 2**-The aircraft approach a potentially unsafe situation. The system will be required to make a fixed-recourse decision upon hitting the switching-state

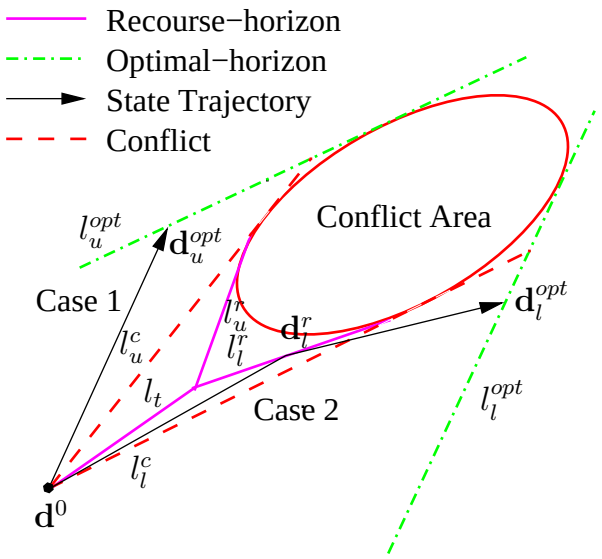

Figure 5: Possible outcomes for the two-stage stochastic model

defined by the recourse-horizon lines, l_u^r or l_l^r. The aircraft will continue along the new trajectory defined by the fixed recourse decision until the state trajectory intersects an optimal-horizon line.

Both trajectories listed above can be described by a sequence of states which the system passes through. Let d_u^{opt} be the switching-state that lies on the upper-optimal-horizon line, and d_l^r be the switching-state that lies on the lower-recourse-horizon line, with the remaining states named similarly. Examples of the states are identified in Fig. 5. The possible processes are listed below, with the first two trajectories corresponding to Case 1, and the last two trajectories corresponding to Case 2.

1. $\mathbf{d}^0 \rightarrow \mathbf{d}_u^{opt}$
2. $\mathbf{d}^0 \rightarrow \mathbf{d}_l^{opt}$
3. $\mathbf{d}^0 \rightarrow \mathbf{d}_u^r \rightarrow \mathbf{d}_u^{opt}$
4. $\mathbf{d}^0 \rightarrow \mathbf{d}_l^r \rightarrow \mathbf{d}_l^{opt}$

Using the above state trajectories, the cost function can be expressed as the sum of the expected cost of any conflict resolution decision over the possible outcomes. This requires that the expected cost over each link along the state trajectory be calculated. First, however, the placement of the optimal-horizon and recourse-horizon lines needs to be described.

The optimal-horizon lines and the recourse-horizon lines need to be calculated for the two-stage stochastic program. We define these lines based on the α-bound on the maximum acceptable probability of conflict, similar to the single-stage model. For the tangent lines l_u^{opt}, l_l^{opt}, l_u^r, and l_l^r, the slopes are sufficient to define the equation of the lines for any given ellipse. In reference to a general tangent line, l^*, we use l^* and m^* interchangeably.

In the single-stage case presented in (14), the α-bound defined the feasible space. This is equivalent to defining the maximum allowable probability of conflict before reaching the optimal-horizon line. For the recourse case, the recourse-horizon line is arbitrarily defined by dividing the probability of conflict equally between both trajectory segments: following the initial resolution-command, and after the recourse-command. Let $P_{r,1}$ be the probability that recourse is required, and let $P_{r,2}$ be the probability of conflict even after the recourse action is taken. According to the α-bound, it then follows that $P_{r,1}P_{r,2} \leq \alpha$. For simplicity, let maximum probability of conflict for the fixed recourse action be $P_{r,2} = \sqrt{\alpha}$. Therefore, the feasible $\mathbf{v}^+$ is defined accordingly:

$$\mathbf{v}^+ \in \left\{(v_1,v_2)|P(m_l^c \leq m \leq m_u^c|v_1^+ = v_1, v_2^+ = v_2) \leq \sqrt{\alpha}\right\} \tag{15}$$

We assume that if the state trajectory of the system reaches the recourse-horizon line, it will switch to the fixed recourse extrema airspeeds to prevent conflict. Based on this assumption, the recourse-horizon lines can then be defined by the slopes:

$$\begin{aligned} m_u^r &= inf\left\{m|P(M < m|v_1 = v_1^{min}, v_2 = v_2^{max}) \leq \sqrt{\alpha}\right\} \\ m_l^r &= sup\left\{m|P(M > m|v_1 = v_1^{max}, v_2 = v_2^{min}) \leq \sqrt{\alpha}\right\} \end{aligned} \tag{16}$$

In this manner, the total maximum probability of conflict to reach the optimal-horizon line is bounded by α.

The optimal-horizon lines are defined in a similar manner. Arriving at the optimal-horizon line the aircraft switch to their desired airspeed. The probability of conflict following the switch should be bounded by α. The optimal-horizon lines are then defined by the slopes:

$$\begin{aligned} m_u^{opt} &= inf\left\{m|P(M < m|v_1 = v_1^{opt}, v_2 = v_2^{opt}) \leq \alpha\right\} \\ m_l^{opt} &= sup\left\{m|P(M > m|v_1 = v_1^{opt}, v_2 = v_2^{opt}) \leq \alpha\right\} \end{aligned} \tag{17}$$

Optimization Model

The optimization within this two-stage framework involves minimization of a cost function. In this section, explicit derivations of the cost function are detailed through the use of standard probability theory. Ultimately, through a series of tightly bounded approximations, followed by numerical integration, the model is shown to be solved in decision-time.

As noted previously, the conflict problem is considered terminated when the state of the system reaches the conflict-free optimal-horizon line. We define the cost function, $G(\mathbf{v}^+)$, as a measure of the expected fuel-disruption to the aircraft,

$$G(\mathbf{v}^+) = \mathbf{E}[C_1] + \mathbf{E}[C_2] \tag{18}$$

where $\mathbf{E}[C_1]$ and $\mathbf{E}[C_2]$ are the individual expected fuel-costs for each aircraft prior to reaching an optimal-horizon line. The process by which the aircraft reaches an optimal-horizon line determines the exact costs. The optimization model requires the minimization of (18) subject to the feasibility requirements described in (15).

Without loss of generality, we first consider aircraft AC_1. Similar results can be expanded to AC_2. The expected cost for AC_1 can be broken down into four segments according to which optimal-horizon line or recourse-horizon line the state trajectory intersects:

$$\mathbf{E}[C_1] = \mathbf{C}_{1,M\otimes l_u^{opt}} + \mathbf{C}_{1,M\otimes l_l^{opt}} + \mathbf{C}_{1,M\otimes l_u^r} + \mathbf{C}_{1,M\otimes l_l^r} \tag{19}$$

where "cross-notation" $M \otimes l_g$ indicates that the state-trajectory intersects the horizon-line l_g. The term $\mathbf{C}_{1,M\otimes l_g}$ is given by:

$$\mathbf{C}_{1,M\otimes l_g} = \mathbf{E}[C_1|M \otimes l_g]P(M \otimes l_g) \tag{20}$$

The value of $P(M \otimes l_g)$ is dependent on the initial configuration of the problem and the planned airspeeds.

We begin to determine the structure of each expectation in (19) by calculating the expected fuel-cost for a planned airspeed $\mathbf{v}^+$ over a given segment s, which is determined by the random variable M. We then integrate over the space of M. The cost over a generic segment s is:

$$\begin{aligned} \mathbf{E}[C_1^s|\mathbf{v}^+, s] =& F_1^{fuel}(v_1^+)\mathbf{E}[T_1|\mathbf{v}^+, s] \\ =& F_1^{fuel}(v_1^+)d_1^s\mathbf{E}[1/V_{1,g}|\mathbf{v}^+, s] \end{aligned} \tag{21}$$

where $F_1^{fuel}(v_1^+)$ [Kg/min] is the fuel-burn function, T_1 is the travel time, d_1^s is the distance traveled over the segment, and $V_{1,g}$ is the random variable describing the groundspeed of the aircraft. The distribution of $V_{1,g}$ is defined according to (9). For a fixed m in the sample space of M, the distribution of the ground speed is normal, i.e., $V_{1,g} \sim \mathcal{N}\left(\hat{v}_{2,g}/m, (r_2/m)^2\right)$, where:

$$V_{1,g} = V_{2,g}/m \tag{22}$$

To evaluate $\mathbf{E}[1/V_{1,g}|\mathbf{v}^+, s]$ over the distribution (22) we can make use of a tight Taylor series approximation [16], [17]. We define a new random variable $Z = 1/V_{1,g}$ and take the Taylor series expansion about $a = \hat{v}_{2,g}/m$:

$$Z = \sum_{k=0}^{\infty} \frac{g^{(k)}(a)\left(V_1^{gs} - a\right)^k}{k!} \tag{23}$$

Taking the expectation of (23), and noting $\mathbf{E}[(V_1^{gs} - a)^n]$ is the n^{th} moment over the normal distribution, the Taylor series can be rewritten as:

$$\mathbf{E}[Z] = m\left[\left(1 + \left(\frac{r_2}{\hat{v}_{2,g}}\right)^2 + \frac{1}{2}\left(\frac{r_2}{\hat{v}_{2,g}}\right)^4 + \ldots\right)/\hat{v}_{2,g}\right] \tag{24}$$

The series converges quickly for the range of values we are considering. Note that we are making the assumption $\mathbf{E}[(V_1^{gs} - a)^n] = \mathbf{E}[(V_1^{gs} - a)^n | V_1^{gs} \geq 0]$, since we assume $P(V_1^{gs} \leq 0) \sim 0$. Letting $A(\hat{v}_{2,g}, r_2)$ equal the summation of the infinite series, and then evaluating the expected cost in Eq. (21), we get:

$$\mathbf{E}[C_1|\mathbf{v}^+, s] = F_1^{fuel}\left(v_1^+\right) d_1^s m A(\hat{v}_{2,g}, r_2) \tag{25}$$

Similarly, the same process applied to the expected fuel-cost for AC_2 yields:

$$\mathbf{E}[C_2|\mathbf{v}^+, s] = F_2^{fuel}\left(v_2^+\right) \frac{d_2^s}{m} A(\hat{v}_{1,g}, r_1) \tag{26}$$

The values of d_1^s and d_2^s, the distance traveled for each aircraft, have yet to be defined. They are in fact random variables. Figure 6 is a pictorial representation of a general case with an arbitrary horizon-line and initial starting point. The values d_1^s and d_2^s are functions of m, the initial aircraft positions, $\mathbf{d}^i = [x_i, y_i]$, and the line in question, l^*. For AC_1 and a general line $l^*(m^*, b^*)$, the distance traveled is given by:

$$d_1^s = \frac{m^* x_i + b^* - y_i}{m - m^*} \tag{27}$$

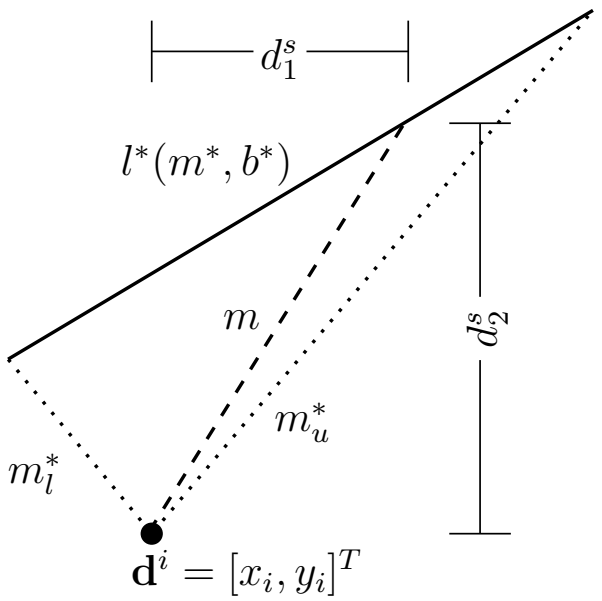

Figure 6: Representation to calculate the distance traveled by the aircraft

and for AC_2, the distance is:

$$d_2^s = \frac{m(m^* x_i + b^* - y_i)}{m - m^*} \tag{28}$$

Now, for the case in which the initial state trajectory intersects the optimal-horizon line, i.e., when no second stage recourse is required, Eq. (25) and (26) can be substituted directly into their respective costs in Eq. (19). As shown in Fig. 5, the range of m for which this will occur is $[max(m_u^c, m_u^{opt}), \infty)$ and $(-\infty, min(m_l^c, m_l^{opt})]$. Integrating the expected cost for both aircraft over this range, for a given $\mathbf{v}^+$, we get:

$$\begin{aligned}
\mathbf{C}_{1,M\otimes l_u^{opt}} &= F_1^{fuel}(v_1^+)A(\hat{v}_{2,g}, r_2)K(l_u^{opt}, \mathbf{d}^0) \\
&\quad \cdot \int_{max(m_u^c, m_u^{opt})}^{\infty} \frac{m}{m - m_u^{opt}} \cdot dF_M(m) \\
\mathbf{C}_{1,M\otimes l_l^{opt}} &= F_1^{fuel}(v_1^+)A(\hat{v}_{2,g}, r_2)K(l_l^{opt}, \mathbf{d}^0) \\
&\quad \cdot \int_{-\infty}^{min(m_l^c, m_l^{opt})} \frac{m}{m - m_l^{opt}} \cdot dF_M(m) \\
\mathbf{C}_{2,M\otimes l_u^{opt}} &= F_2^{fuel}(v_2^+)A(\hat{v}_{1,g}, r_1)K(l_l^{opt}, \mathbf{d}^0) \\
&\quad \cdot \int_{max(m_u^c, m_u^{opt})}^{\infty} \frac{1}{m - m_u^{opt}} \cdot dF_M(m) \\
\mathbf{C}_{2,M\otimes l_l^{opt}} &= F_2^{fuel}(v_2^+)A(\hat{v}_{1,g}, r_1)K(l_l^{opt}, \mathbf{d}^0) \\
&\quad \cdot \int_{-\infty}^{min(m_l^c, m_l^{opt})} \frac{1}{m - m_l^{opt}} \cdot dF_M(m)
\end{aligned} \tag{29}$$

where,

$$K(l^*, \mathbf{d}^i) = (m^* x_i + b^* - y_i) \tag{30}$$

The line l_t is defined as the line connecting $\mathbf{d}^0$ and the intersection point between l_u^r and l_l^r, as shown in Fig.

5. For the case where recourse is required, in particular when the state trajectory intersects the upper-recourse-horizon line, a similar calculation can be performed. The expected cost for this case can then be expressed as:

$$\begin{aligned}\mathbf{C}_{1,M\otimes l^r} = \; & F_1^{fuel}(v_1^+)A(\hat{v}_{2,g},r_2)K(l_u^{rc},\mathbf{d}^0) \\ & \cdot \int_{m_t}^{min(m_u^c,m_u^r)} \frac{m_1}{m_1-m_u^r}\cdot dF_{M_1}(m) \\ & + F_1^{fuel}(v_1^{min})A(\hat{v}_{2,g}^r,r_2) \\ & \cdot \int_{m_l^c}^{m_u^c} K(l_u^{opt},\mathbf{d}_u^r) \\ & \cdot \int_{max(m_u^r,m_u^{opt})}^{\infty} \frac{m_2}{m_2-m_u^{opt}}\cdot dF_{M_2}(m)\cdot dF_{M_1}(m)\end{aligned} \tag{31}$$

where the first integral accounts for the first-stage costs, and the second integral is a measure of the recourse costs.

This process can be repeated for AC_2, as well as for intersections with the lower-recourse-horizon for both aircraft. These additional costs are then used to complete the definition of the cost function in (18).

Computational Analysis

Given the complexity of the cost function, it is quite difficult to assess the properties of the formulation from an analytical perspective. The cost function is neither convex nor quasi-convex over the complete space, even when the space is partitioned in half according to $\hat{m}^+ \geq m_u^c$ and $\hat{m}^+ \leq m_l^c$. Hence, an analytical solution to the problem cannot be derived, and numerical methods need to be used. On the other hand, numerical evaluations over the feasible space can be performed in a very fast and efficient manner.

The cost function requires numerical methods to evaluate a number of integrals over a series of conflict resolution commands, $\mathbf{v}^+$. For the computational cost to evaluate a single instance of the integral of the form $\int_{m_l}^{m_u} f(m)dF_M(m)$, we assume that a discretization of the probability distribution with κ_m values over the space is used. Let the space of v_1^+ be discretized at μ values, and v_2^+ be discretized at ν values over their range. The upper-bound on the total number of required evaluations of the integral is given by $6\mu\nu$, corresponding to $4\mu\nu$ evaluations in (29) and $2\mu\nu$ evaluations in (31) for each (v_1^+, v_2^+) pair. An additional fixed number of evaluations are required to calculate the recourse cost, which is an inner integral in (31). The feasible space is determined through evaluation of the cumulative distribution function. As a result, the complexity of the numerical evaluation procedure is $O(\mu\nu\kappa_m)$.

The procedure was implemented in Matlab using a single processing-core of a quad-core 2.66 GHz computer with 2GB of memory, and was observed to run in decision-time in all cases. As an example, at a grid spacing of $\delta v = 5$ over a range of $[400,600]$ kts for each aircraft, and integrating over the space of M within the two-tailed α-bound of $1/1000^2$, corresponding to $m \in [.5743, 1.7410]$ with $\delta m = 1/1000$, the value of the cost function over the complete space was calculated in 2.3 seconds. Clearly, even faster implementations are possible in other programming environments. Furthermore, the calculations are well suited for evaluation using multiple processor-cores to improve run-time linearly.

Simulation results

A sample result is provided to develop some intuitive understanding of the formulation and cost function. The following initial conditions were defined for a test case:

- $D_{min} = 5NM$
- $\theta = 90^o$
- $\mathbf{d}^0 = [-70, -70]$
- $v_1^+ \in [400, 600]$
- $v_1^{opt} = 500$
- $v_2^+ \in [370, 570]$
- $v_2^{opt} = 470$
- $\hat{v}_{i,w} = 0$
- $r_1 = r_2 = .25$
- $\rho = .15$

For this case, we assumed a simple fuel cost function for each aircraft, defined as $F_i^{fuel} = (v_i^{opt} - v_i^+)^2$. The cost function (18) was evaluated over a meshgrid with spacing of $\delta v = 5$. The total expected cost for the problem when the state trajectory intersects the optimal-horizon line is shown in Fig. 7. As expected, the more conservative maneuvers result in increased costs. However, for more risky actions when the aircraft maintain desired speeds, $v_1^{opt} = 500$ and $v_2^{opt} = 470$, the expected costs are also low. The low expected cost in this region is to be expected as a result of (20) since the probability still hitting a optimal-horizon line is low. In fact, if the aircraft maintains airspeeds close to the desired or optimal airspeeds, increasing the probability of taking recourse actions, the expected costs due to required recourse actions is larger, as shown in Fig. 8.

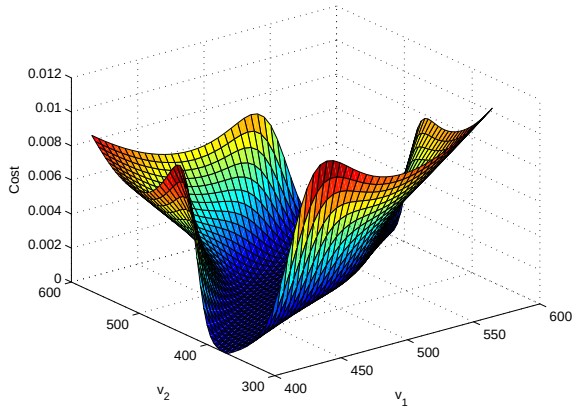

Figure 7: Expected cost when state trajectory intersects l^{opt}

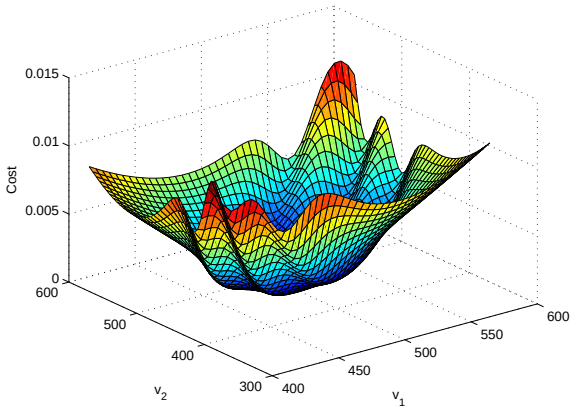

Figure 9: Cost function evaluated over the domain

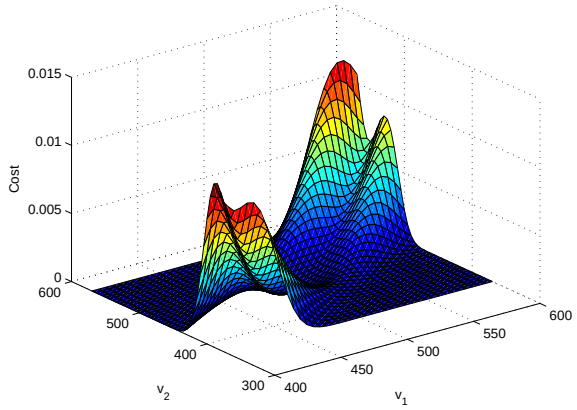

Figure 8: First and second-stage expected costs when state trajectory intersects l^r

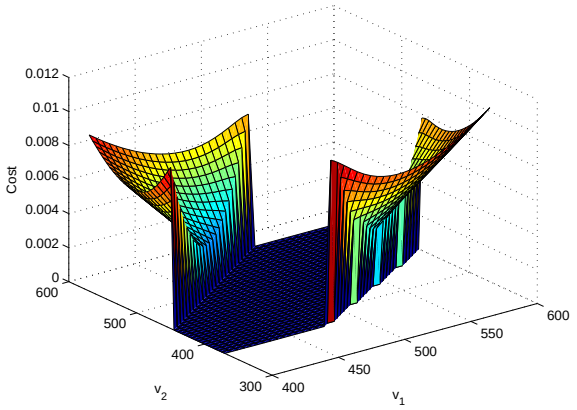

Figure 10: Cost function over the feasible space

The complete cost function $G(\mathbf{v}^+)$, involving all possible trajectories and evaluated over the entire space is shown in Fig. 9. The cost function is again shown in Fig. 10, but this time only over the feasible space. Note that the function is nonconvex, eliminating the possibility of using standard gradient search methods to achieve guaranteed convergence to a global optimum. Hence, an enumerative evaluation procedure is necessary. As discussed, such a procedure can be performed in real-time and an optimal solution can be identified. For this example, identifying the mimimium cost results in the speed assignments of $v_1^+ = 520$ knots and $v_2^+ = 435$ knots.

Conclusions and future work

In an environment where uncertainty is ever present, and decisions are both safety-critical and cost-conscience, there is a need for realistic tools to aid air traffic controllers. In this paper we have presented a formulation for a two-stage stochastic program for air traffic conflict resolution with speed changes. The formulation's aim is to consider the issue of wind uncertainty in air traffic resolution. Furthermore, the formulation goes beyond a simple single-stage optimization model, and does not extend to resolve the stochastic problem continuously. In this manner, the model developed is both robust and practical, as it provides fixed limits on the workload and the amount of decision-making required by air traffic controllers. More specifically, an initial resolution command is issued, and a fixed recourse is provided as needed. And more so, the recourse decision can be automated without input from the controller.

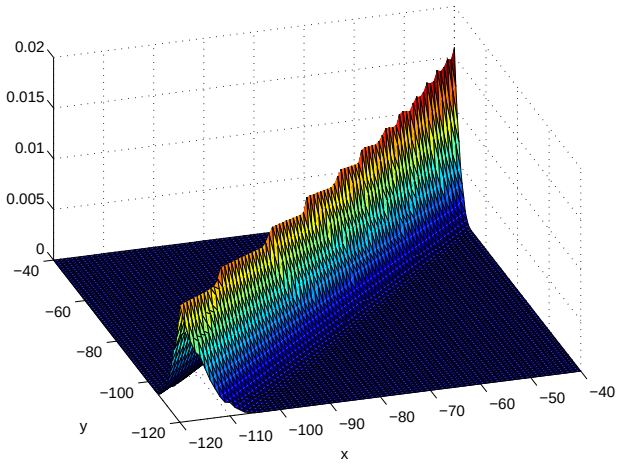

Figure 11: Cost-to-go solution for various initial conditions

This research is a first-step in answering the question, "When should conflicts be resolved?" In Fig. 11 a cost-to-go map is shown for a problem similar to that described in the Simulation section, with the conflict resolution problem solved over a range of initial distances. In this case, the intersection angle $\theta = 90^o$, and the two aircraft have the same desired airspeed $v_{i,d} = 500$. Given the cost-to-go map, based on current positions, airspeeds, and wind properties, it will be possible to calculate the cost of issuing a resolution command at the present time, or waiting until a more beneficial time.

Lastly, there is a need to compare speed-change resolution commands against heading-change resolutions. Future work involves the development of a similar two-stage model with heading-change commands.

Acknowledgments

This work is funded by NASA under Grant NNX08AY52A and by the FAA under Award No.: 07-C-NE-GIT, Amendment Nos. 005, 010, and 020

References

[1] J. Kuchar and L. Yang, "A review of conflict detection and resolution modeling methods," *IEEE Transactions on Intelligent Transportation Systems*, vol. 1, pp. 179–189, Dec. 2000.

[2] K. Blin, M. Akian, E. Hoffman, M. Claude, and K. Zeghal, "A stochastic conflict detection model revisited," in *Proc. of AIAA Guidance, Navigation, and Control Conference and Exhibit*, August 2000.

[3] D. Karr and R. Vivona, "Conflict detection using variable four-dimensional uncertainty bounds to control missed alerts," in *Proc. of AIAA Guidance, Navigation, and Control Conference and Exhibit*, August 2006.

[4] C. van Daalen and T. Jones, "Fast conflict detection using probability flow," *Automatica*, June 2009.

[5] J. K. Kuchar and L. C. Yang, "Incorporation of uncertainty intent information in conflict detection and resolution," in *Proc. of the 1997 Conference on Decision and Control (CDC'97)*, December 1997.

[6] J. Hu, J. Lygeros, M. Prandini, and S. Sastry, "Aircraft conflict prediction and resolution using brownian motion," in *Proc. of the 1999 Conference on Decision and Control (CDC'99)*, December 1999.

[7] L. Blackmore, H. Li, and B. Williams, "A probabilistic approach to optimal robust path planning with obstacles," in *Proc. 2006 American Control Conference (ACC'06)*, pp. 2831–2837, June 2006.

[8] L. Wojcik, "Probabilistic aircraft conflict analysis for a future air traffic management system," *Journal of Aerospace Computing, Information, and Communication*, vol. 6, no. 6, pp. 393–404, 2009.

[9] R. Irvine, "A geometrical approach to conflict probability estimation," *Air Traffic Control Quarterly*, vol. 10, no. 2, pp. 85–113, 2002.

[10] R. A. Paielli and H. Erzberger, "Conflict probability estimation for free flight," *Journal of Guidance, Control, and Dynamics*, vol. 20, no. 3, pp. 588–596, 1997.

[11] R. Irvine, "A simplified approach to conflict probability estimation," in *Proc. of the 20th Digital Avionics Systems Conference*, vol. 2, pp. 7F5/1–7F5/12, 2001.

[12] C. Wanke, "Using Air-Ground Data Link to Improve Air Traffic Management Decision Support System Performance," in *USA-Europe ATM R&D Seminar*, 1997.

[13] S. Mondoloni, "A Multiple-Scale Model of Wind-Prediction Uncertainty and Application to Trajectory Prediction," in *Proc. of the* 6*th AIAA Aviation Technology, Integration and Operations Conference*, pp. 7807–7820, 2006.

[14] W. Glover and J. Lygeros, "A multi-aircraft model for conflict detection and resolution algorithm evaluation," *European Hybridge Project, Tech. Rep*, 2004.

[15] D. Hinkley, "On the ratio of two correlated normal random variables," *Biometrika*, vol. 56, pp. 635–639, 1969.

[16] J. Rice, *Mathematical Statistics and Data Analysis*. Duxbury Press, 1995.

[17] S. Solak, J.-P. Clarke, and E. Johnson, "Airport terminal capacity planning," *Transportation Research Part B*, vol. 43, no. 6, pp. 659–676, 2009.

Email Addresses

Adan Vela: aevela@gatech.edu,
Erwan Salaün: erwan.salaun@gatech.edu,
Senay Solak: solak@som.umass.edu,
Eric Feron: feron@gatech.edu.
William Singhose: singhose@gatech.edu,
John-Paul Clarke: johnpaul@gatech.edu,

28th Digital Avionics Systems Conference
October 25-29, 2009